Japanese Journal of Applied Physics
Vol. 43, No. 11B, 2004, pp. L 1488–L 1491

Eddy-Current-Based Nondestructive Inspection System Using Superconducting Quantum Interference Device for Thin Copper Tubes

Yoshimi HATSUKADE*, Akifumi KOSUGI, Kazuaki MORI[1] and Saburo TANAKA

Toyohashi University of Technology, 1-1 Hibarigaoka, Tempaku-cho, Toyohashi, Aichi 441-8580, Japan
[1]*Sumitomo Light Metal Industries, Ltd., Copper Works, 100 Ougishinmichi, Ichinomiya-cho, Hoi-gun, Aichi 441-1295, Japan*

(Received July 9, 2004; accepted September 15, 2004; published October 29, 2004)

An eddy-current-based nondestructive inspection (NDI) system using superconducting quantum interference device (SQUID) cooled using a coaxial pulse tube cryocooler was constructed for the inspection of microflaws on copper tubes employing a high-T_c SQUID gradiometer and a Helmholtz-like coil inducer. The detection of artificial flaws several tens of μm in depth on copper tubes 6.35 mm in outer diameter and 0.825 mm in thickness was demonstrated using the SQUID-NDI system. With an excitation field of 1.6 μT at 5 kHz, a 30-μm-depth flaw was successfully detected by the system at an SN ratio of at least 20. The magnetic signal amplitude due to the flaw was proportional to both excitation frequency and the square of flaw depth. With consideration of the system's sensitivity, the results indicate that sub-10-μm-depth flaws are detectable by the SQUID-NDI system. [DOI: 10.1143/JJAP.43.L1488]

KEYWORDS: nondestructive inspection, microflaws, copper tube, high-T_c SQUID, gradiometer, eddy current

For greater performance, the thickness of thermal-exchange copper tubes has tended to decrease in recent years. Thus, microflaws less than several tens of μm in depth have become serious problems that cause tube breakage and coolant leakage in post processes. Concerning nonmagnetic metal tubes, eddy current testing (ECT) has been mainly applied to the detection of flaws in thermal-exchange tubes.[1)] However, there is a limit to the ability of ECT to detect small flaws. At present, the minimum limit of detectable flaw depth by commercial ECT on the market is about 50–100 μm.[1–3)] Thus, a more sensitive detection technique is strongly desired in both quality control and economic aspects.

A high-T_c superconducting quantum interference device (SQUID) is an extremely sensitive magnetic sensor.[4)] Because of their great sensitivity from DC to several 100 kHz, high-T_c SQUIDs have been applied to the nondestructive inspection (NDI) of various materials and structures. Thus far, the objects inspected by SQUID-NDI are nonmagnetic metals,[5–7)] carbon-fiber composites,[8–11)] and cables with ferromagnetic inclusions.[12)] By an eddy-current-based technique, NDI using SQUID (SQUID-NDI) has superior ability to detect small flaws in conductive materials without contact.[5–7,9,10)] In this paper, we describe a cryocooler-cooled SQUID-NDI system for the inspection of copper tubes. The detection of surface flaws several tens of μm in depth on the tubes was demonstrated using the SQUID-NDI system.

We constructed a SQUID-NDI system cooled by a coaxial pulse tube cryocooler (PTC) for metallic and composite board materials.[10)] For the inspection of tubes, a Helmholtz-like coil is employed as an eddy current inducer.[13)] In the lengthening and thinning of the copper tubes, flaws on the tubes are also lengthened along the axis of tube and thinned. To detect such shallow flaws, a Helmholtz-like coil is suitable because it induces eddy current circulating around the circumference of the tube (perpendicular to the axis of tube) when the tube passes through the coil. The schematic image of the eddy current induced in tube under test is illustrated in Fig. 1(a). The SQUID, which is located between field coils of the Helmholtz-like coil and above the tube, measures the magnetic anomaly generated by the eddy current, which is disturbed by microflaws on the tube surface.

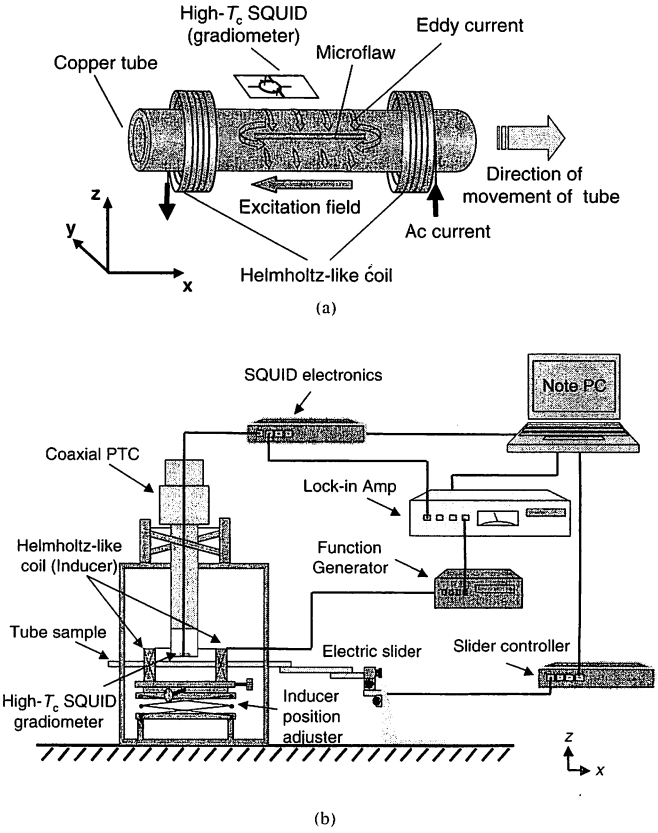

Fig. 1. (a) Principle of detection of microflaws on tube using high-T_c SQUID and Helmholtz-like coil. (b) Schematic drawing of cryocooler-cooled SQUID-NDI system for inspection of tube.

Figure 1(b) shows the schematic drawing of the SQUID-NDI system with the Helmholtz-like coil. A high-T_c SQUID gradiometer has been employed for decreasing of ambient magnetic noise for operation in a magnetically unshielded environment. The use of a gradiometer also enables the construction of a low-noise cryocooler-cooled system without a significant increase in noise. The dimensions of a one-

*Corresponding author. E-mail address: hatukade@eco.tut.ac.jp

sided pick-up coil and the length of the baseline (distance between the centers of the pick-up coils) of the gradiometer are 3.5 mm × 3.5 mm, and 3.5 mm, respectively. A compact coaxial PTC was introduced to cool the SQUID down to approximately 77 K. Details of the PTC and SQUID are described elsewhere.[10] The magnetic flux noise of the SQUID-NDI system measured in a flux-locked loop (FLL) operation is about $80\,\mu\phi_0/\mathrm{Hz}^{1/2}$ from 10 Hz to 5 kHz, where $\phi_0 = 2.07 \times 10^{-15}$ Wb is the magnetic flux quantum. Two field coils are connected in series to form the Helmholtz-like coil. The turn number and dimensions of each field coil are 3000, and 48 mm in diameter and 42 mm in length, respectively. The field coils are arranged with a distance of 44 mm between each coil end. The electric slider driven by a stepper motor moves the tube through the Helmholtz-like coil. The function generator supplies ac current into the Helmholtz-like coil, to induce eddy current in the tube sample. The lock-in amplifier measures the output signal from SQUID electronics. The note PC controls the electric slider and obtains the data through the lock-in amplifier.

We prepared three copper tube samples that have artificial shallow flaws with various depths on their surfaces. The dimensions of all the tubes are 6.35 mm in outer diameter, 0.825 mm in thickness and 300 mm in length. The flaws are 100 μm in width and 15 mm in length. The depths of the flaws are different: 100 μm, 50 μm, and 30 μm. These flaws were made using an electric discharge machine.

We performed two types of measurement: one with an excitation field at 440 Hz, and the other with an excitation field at 5 kHz. A sinusoidal current of 80 μA was supplied to the Helmholtz-like coil. The coils generate an excitation field B_x of 1.6 μT at the center of the field coils with a current of 80 μA. The tube samples were passed through the center of the Helmholtz-like coils at a speed of 12 mm/s along the x-axis as shown in Fig. 1. The flaws on the tube samples were oriented to be closer to the SQUID gradiometer that was located above the sample with a lift-off distance (distance between the SQUID and the sample surface) of 1.5 mm. The SQUID gradiometer measured the gradient in the x component of the vertical magnetic field, dB_z/dx (See Fig. 1(a)). The position of the SQUID was carefully adjusted relative to the Helmholtz-like coil to minimize the SQUID output due to the excitation field. The sampling interval along x-axis was 0.3 mm.

The measurement results on the tube samples with 100-μm-, 50-μm-, and 30-μm-depth flaws using the excitation field at 440 Hz are shown in Figs. 2(a)–2(c). For comparison, a *flawless* tube sample of the same dimensions was also measured. The result of the flawless sample is superposed in Fig. 2(a). In each figure, a couple of downward arrows indicate flaw ends. In Fig. 2(a), two pairs of anomalous signal peaks (upward and downward) due to the 100-μm-depth flaw appear above both the flaw ends. The distance between the peaks in each pair is about 5 mm. This distance should be determined by the dimensions of pick-up coils (7 mm × 3.5 mm), which is larger than the list-off distance (1.5 mm). The anomalous signals due to the 50-μm- and 30-μm-depth flaws are also observed as shown in Fig. 2(b) and (c), but the signal-to-noise (SN) ratios of these signals are much poorer than that due to the 100-μm-depth flaw.

On the other hand, the results of the same samples with an excitation field at 5 kHz are shown in Figs. 3(a)–3(c). At a higher frequency excitation field, all anomalous signals due to the flaws were accurately measured. As shown in Fig. 3(c), the 30-μm-depth flaw was successfully detected

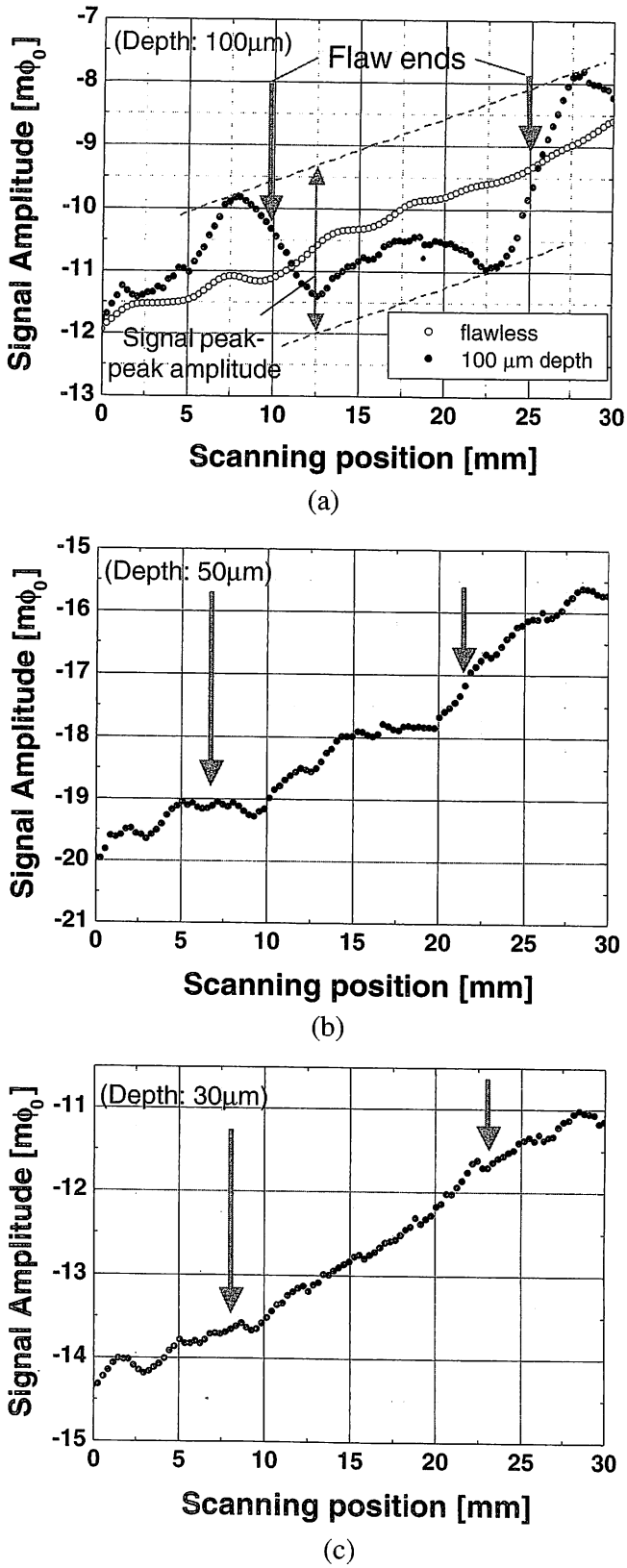

Fig. 2. Experimental results for 440 Hz excitation field of (a) 100-μm-depth flaw, (b) 50-μm-depth flaw, and (c) 30-μm-depth flaw. For comparison, the result of a flawless tube sample of the same dimensions is superposed in Fig. 2(a).

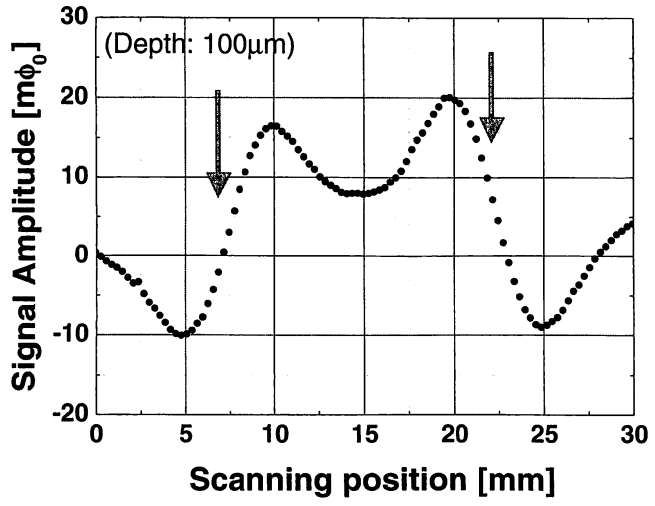

(a)

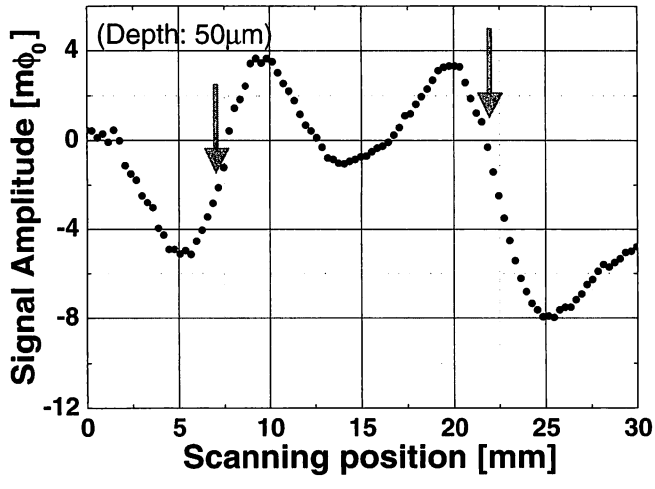

(b)

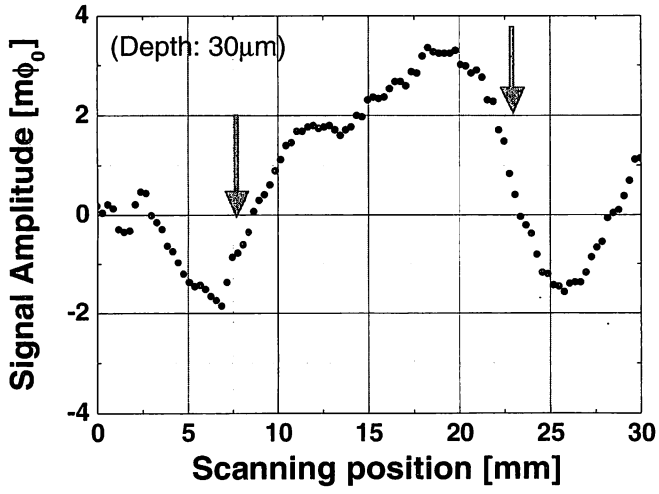

(c)

Fig. 3. Experimental results for 5 kHz excitation field of (a) 100-μm-depth flaw, (b) 50-μm-depth flaw, and (c) 30 μm-depth flaw. In all graphs in Figs. 2 and 3, the bold downward arrows indicate the positions of flaw ends.

with an SN ratio of at least 20, which conventional ECT should fail to detect. The slantwise offset outputs observed in Fig. 2 are due to edge effects. In contrast, edge effects are faintly observed in Fig. 3 mainly because of larger longitudinal scaling.

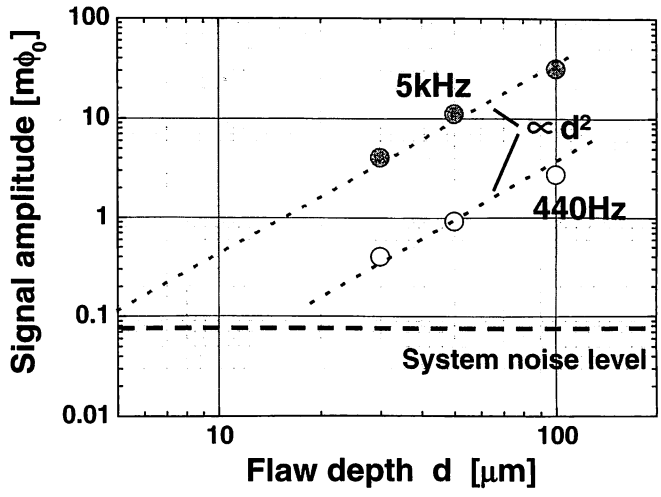

Fig. 4. Signal peak-peak amplitude due to flaw as function of flaw depth d. Signal amplitude is proportional to the square of the flaw depth at both excitation frequencies. The system noise level is also shown by a horizontal dashed line.

Figure 4 shows the relationship between the peak-peak amplitude of the magnetic signal due to the flaw and flaw depth obtained from the results shown in Figs. 2 and 3. We defined the peak-peak amplitude as shown in Fig. 2(a) with consideration of edge effects, because the field gradient due to edge effects was roughly linear. In both cases of 440 Hz excitation and 5 kHz excitation, signal amplitude decreases by a factor of d^2 as flaw depth decreases, where d is the flaw depth. At the same flaw depth, the signal amplitude in 5 kHz excitation is about 10 times larger than that in 440 Hz excitation. This indicates that signal amplitude is proportional to excitation frequency. It is thought that this proportional relationship between signal amplitude and excitation frequency should be maintained unless the skin depth δ becomes much less than the thickness of the tube sample; in this case, δ of copper with a 5 kHz excitation field is about 0.95 mm.

Here, we discuss the relationship between signal amplitude and flaw depth shown in Fig. 4. Since the pair of the anomalous signal peaks appears above the flaw ends, these peaks should be caused by the disturbed current near the flaw ends. Figure 5 shows the schematic image of the flows

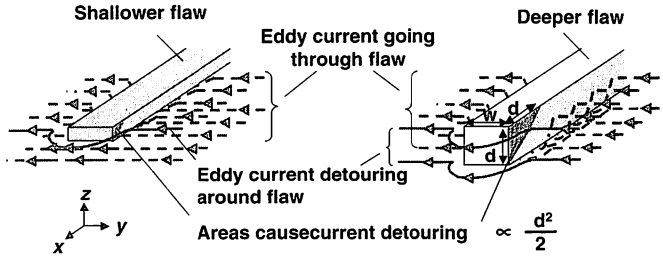

Fig. 5. Schematic illustrations of flows of eddy currents near one end of flaw. It is assumed that the length of the flaw is much larger than the width w and depth d of the flaw, and d is equal to or less than w. The currents far from a flaw end must go through the flaw, while the currents oriented toward the dark dotted triangular area (equal to $d^2/2$) must detour around the flaw.

of the eddy currents near one end of a flaw. The dotted rectangular areas and the arrows indicate the flaws on the specimens and the eddy currents, respectively. It is assumed that the length of the flaw is much larger than the width w and depth d of the flaw, and d is equal to or less than w. Also, the eddy currents are assumed to be flowing perpendicular to the lengths of the flaws. As shown in Fig. 5, the currents far from the flaw ends must pass under a flaw, while the currents oriented toward the dark triangular area on a flaw must detour around the flaw, according to the minimum energy law. The triangular area, which causes current detouring, is equal to $d^2/2$. Thus, it is thought that the signal peaks due to the detoured currents should be proportional to the square of the flaw depth d as shown in Fig. 4. With consideration of this proportional relationship and the system's noise level shown in Fig. 4, we can conclude that the minimum limit of detectable flaw depth using the SQUID-NDI system is approximately 10 μm in 5 kHz excitation and at an SN ratio of at least 5. To our knowledge, this flaw depth is at least 5 times smaller than the limit of conventional ECT.[1–3)]

In conclusion, we constructed a cryocooler-cooled SQUID-NDI system for the inspection of microflaws on copper tubes employing a Helmholtz-like coil inducer. We demonstrated the detection of artificial flaws several tens of μm in depth using the SQUID-NDI system. With an excitation field of 1.6 μT at 5 kHz, a 30-μm-depth flaw was successfully detected at an SN ratio of at least 20. The signal peak-peak amplitude due to the flaw is proportional to the square of flaw depth and excitation frequency. With consideration of these proportional relationships and the system's sensitivity, the results indicate that sub-10-μm-depth flaws are detectable by the SQUID-NDI system.

To bring this technique to the actual applications, the problems to be overcome are as follows: the high speed transfer of the tubes (generally they move at 200–400 m/min), the vibration of tubes due to the high speed transfer, and electromagnetic interferences from the environment, including those from mechanical machines in factories.

1) A. J. Trivedi and R. R. Parikh: *Proc. 14th World Conf. Non-Destructive Testing* (1996) Vol. 3, p. 1729.
2) K. A. Gopal, N. Raghu, N. G. Muralidharan, P. V. Kumar and K. V. Kasiviswanathan: *Proc. 14th World Conf. Non-Destructive Testing* (1996) Vol. 2, p. 663.
3) A. Fedorov, V. Popov, V. Gorsky and A. A. Bochvar: *Proc. 14th World Conf. Non-Destructive Testing* (1996) Vol. 3, p. 1709.
4) *Principle and Application of Superconducting Quantum Interference Devices*, ed. A. Barone (World Scientific, Singapore, 1992) p. 64.
5) A. Cochran, G. B. Donaldson, L. N. C. Morgan, R. M. Bowman and K. J. Kirk: British J. NDT **35** (1993) 173.
6) Y. Tarvin, H.-J. Krause, W. Wolf, V. Glyantsev, J. Schubert, W. Zander and H. Bousack: Cryogenics **36** (1996) 83.
7) R. Hohmann, M. Maus, D. Lomparski, M. Greuneklee, Y. Zhang, H.-J. Krause, H. Bousack and A. I. Braginski: IEEE Trans. Appl. Supercond. **9** (1999) 3801.
8) Y. Hatsukade, N. Kasai and A. Ishiyama: Jpn. J. Appl. Phys. **40** (2001) L606.
9) Y. Hatsukade, N. Kasai, H. Takashima and A. Ishiyama: Supercond. Sci. Technol. **15** (2002) 1728.
10) Y. Hatsukade, T. Inaba, N. Kasai, Y. Maruno, A. Ishiyama and S. Tanaka: Physica C **412-414** (2004) 1484.
11) Y. Hatsukade, M. S. Aly-Hassan, N. Kasai, H. Takashima, H. Hatta and A. Ishiyama: IEEE Trans. Appl. Supercond. **13** (2003) 207.
12) H. Itozaki, T. Nagaishi, H. Toyoda and H. Kugai: IEICE Trans. Electron **E80-C** (1997) 1247.
13) S. Tanaka, T. Mizoguchi, H. Ota and Y. Kondo: IEICE Trans. Electron **E85-C** (2002) 687.